JOURNAL OF SOLID STATE CHEMISTRY 21, 331–347 (1977)

Crystal Structure and Conductivity of 26-Silver 18-Iodide Tetratungstate, $Ag_{26}I_{18}W_4O_{16}$*

LILIAN Y. Y. CHAN AND SEYMOUR GELLER

Department of Electrical Engineering, University of Colorado, Boulder, Colorado 80309

Received January 24, 1977

$Ag_{26}I_{18}W_4O_{16}$ belongs to space group $C2$ with $Z = 2$ and $a = 16.76 \pm 0.03$, $b = 15.52 \pm 0.03$, $c = 11.81 \pm 0.02$ Å, $\beta = 103.9 \pm 0.3°$. Conductivity measurements have been made on polycrystalline material between 22 and 170°C; the average conductivity at 25°C is 0.059 $(\Omega\,\text{cm})^{-1}$. The conduction passageways involve 90 iodide polyhedra and 56 mixed oxygen–iodide polyhedra (per unit cell) which share faces. An average of 23.2 or 44.5% of the Ag^+ ions per unit cell are in these polyhedra and are considered to be mobile. The Ag^+ ion occupancies of the mixed I–O polyhedra tend to be higher than those of the pure iodide polyhedra, implying that the Ag^+ ion mobilities through the former are lower than those through the latter. Ag^+ ions fill 12 mixed I–O polyhedral sites and 16.8 Ag^+ ions per unit cell are in 24 other mixed I–O bypass sites; these 28.8 Ag^+ ions are probably not mobile. The three-dimensional network of passageways is rather complex, but an attempt is made to give a complete description of it.

Introduction

The crystal structures of several AgI-based solid electrolytes containing cation substituents for Ag^+ have been determined (*1–9*). The first of these for $RbAg_4I_5$ (*1*) led to the first enunciation of the structural origin of the phenomenon of electrolytic conductivity in this type of material (see also Ref. *10*). This has been discussed in several subsequent papers (*2–10*) and, because this paper, even without reiteration of this discussion, is of necessity long, it is assumed that the reader is familiar with the content of those papers.

When the work of Takahashi and coworkers (*11*) on complex anion substituents appeared (*11*, *12*) it seemed appropriate to see what the structural and related conductivity effects of such substitution were, and we therefore first undertook to determine the crystal structure of the silver–iodide–tungstate solid electrolyte reported by Takahashi *et al.* (*11*).

At an early date in this investigation, it was found that the formula $Ag_6I_4WO_4$ reported for this compound could not be correct. Eventually, we determined from single-crystal X-ray data, from conductivity and density measurements, and from the crystal structure solution itself that the correct formula is $Ag_{26}I_{18}W_4O_{16}$. It will be immediately noticed that the *nominal chemical* formula may be written $Ag_{13}I_9(WO_4)_2$; however, this is not an appropriate *structural* formula for the compound.

Because it was not known what tungstate entity would be present in the solid electrolyte which appeared at the outset to have a rather complex low symmetry structure, it was decided to determine the crystal structure of silver tungstate itself. As mentioned elsewhere (*13*), there are two modifications of silver tungstate which form under slightly different pH. They also appear to be thermodynamically stable in different temperature regions. The structure of the high-temperature phase was determined (*13*). It was also found that crystals of this form could be grown by the Czochralski technique (*14*).

The result of the structure determination

* Supported by the National Science Foundation under Grant DMR No. 72-03271-AO1.

ISSN 0022-4596

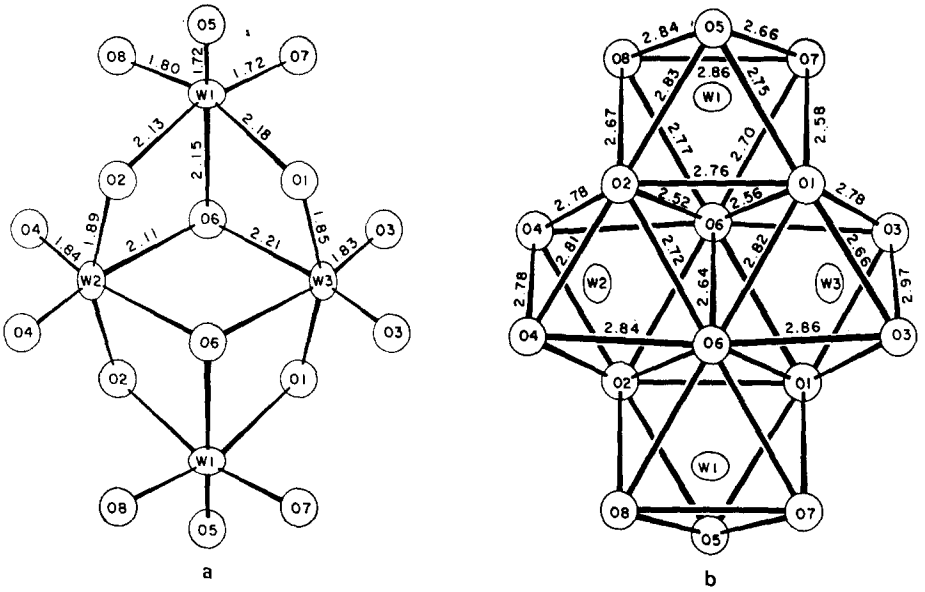

FIG. 1. The $(W_4O_{16})^{8-}$ ion in $Ag_{26}I_{18}W_4O_{16}$: (a) W–O distances, (b) O–O distances. Note that the $(W_4O_{16})^{8-}$ ion in $Ag_{26}I_{18}W_4O_{16}$ is enantiomorphous to that in $Ag_8W_4O_{16}$ (see Ref. (*13*)).

most relevant to this paper is the appearance of a new $(W_4O_{16})^{8-}$ complex as shown in Fig. 1. This complex has point symmetry 2 (or C_2) and is the tungstate entity that occurs in the solid electrolyte.

Conductivity

Experimental

The $Ag_8W_4O_{16}$ used in the preparation of the solid electrolyte was produced by adding a concentrated solution of sodium tungstate to one of silver nitrate in essentially stoichiometric proportions. The precipitate, which is highly insoluble in water, was washed with H_2O (by decantation) approximately 30 times, then filtered through a Büchner funnel and dried in an oven at 110°C.

The *pure* solid electrolyte $Ag_{26}I_{18}W_4O_{16}$ *cannot* be prepared by melting inasmuch as it melts incongruently. *Some* of the compound is obtained by melting, but in this case AgI and the compound with nominal chemical formula $Ag_5I(WO_4)_2$ are always present. (If this compound contains $(W_4O_{16})^{8-}$ entities, which is likely, then its formula should be written $Ag_{10}I_2W_4O_{16}$.) The chemical equation for the decomposition is

$$Ag_{26}I_{18}W_4O_{16} \rightleftarrows 16AgI + Ag_{10}I_2W_4O_{16}.$$

Thus even a slight decomposition causes a large amount of AgI to be present. This gives a sensitive probe for purity of the solid electrolyte with respect to unreacted AgI. The latter *can* be seen in the powder X-ray diffraction photograph, although there are subtleties because of overlap of AgI lines with those of the solid electrolyte (see Appendix). The conductivity measurements are extremely sensitive to the presence of AgI, probably to a small fraction of a percent.

Rapid melting of the thoroughly mixed ingredients in the ratio $4AgI:Ag_2WO_4$ and quenching gives $Ag_{26}I_{18}W_4O_{16}$ plus $Ag_{10}I_2W_4O_{16}$ but no AgI, of course. In this case, the $Ag_{10}I_2W_4O_{16}$ can be detected by powder X-ray diffractometry (see Appendix).

A polycrystalline specimen of the solid electrolyte *cannot* be prepared by *solid state reaction* in a reducing atmosphere! In fact, the preparation requires a substantial overpressure of oxygen because at the reaction temperature of 280°C the solid electrolyte appears to have a relatively high oxygen vapor

pressure. It has been shown recently (*15*) that $Ag_8W_4O_{16}$ itself decomposes on being heated to temperatures exceeding 280°C. However, the solid electrolyte $Ag_{26}I_{18}W_4O_{16}$ appears to be substantially less stable with respect to oxygen than $Ag_8W_4O_{16}$ itself. (Inasmuch as we are primarily interested in obtaining a stoichiometric specimen, we have not expended effort in determining the detailed thermodynamics of the system.) It appeared that two opposing reactions were going on when the oxygen pressure was too low: The reaction of AgI and $Ag_8W_4O_{16}$ to give the solid electrolyte and the decomposition of the solid electrolyte with respect to oxygen. No free iodine was ever observed, so that oxidation of the iodide ion is not involved. We speculate that the main reaction involves removal of oxygen from the tetratungstate ion without necessarily changing its valence. This would require some reduction of the tungsten valences. For example, suppose that the $[W_4O_{16}]^{8-}$ ion went to $(W_4O_{15})^{8-}$. This simply requires a total reduction of 2 in the new valence of the four W atoms; this of course, may be accomplished by having two W^{6+} and two W^{5+}, or three W^{6+} and one W^{4+}. The production of such entities also implies the existence of disorder in the partially reduced crystals. It has also been observed that melting together the AgI and $Ag_8W_4O_{16}$ in vacuum as prescribed by Takahashi *et al.* (*11*) or even melting in air for extended time periods produces *free silver* (but *not free iodine*). This does not occur in the case of silver tungstate alone. Thus it is conceivable that this occurs by a loss of oxygen by some tetratungstate ions (*15*). The reduced tetratungstate ions then in turn reduce Ag^+ ions. Then, somehow, the I^- ions attach themselves to the reoxidized tetratungstate ion. This is only a hypothesis which could explain the observations.

The discussion given above is the result of considerable work on the preparation of the polycrystalline material. The crystal structure gave us assurance that the formula of the solid electrolyte was $Ag_{26}I_{18}W_4O_{16}$, but attempts to make the polycrystalline material for average conductivity measurements at first shook this confidence somewhat (*8*). However, the work led to the realization that an overpressure of oxygen was required. We obtained a single phase specimen as ascertained from both powder X-ray diffraction data and conductivity measurements by the following technique: Amounts of the $Ag_8W_4O_{16}$ prepared as described above and 99.9% AgI (Research Organic-Inorganic Chemicals Co., Grade AR) appropriate to the preparation of 0.005 mole, were ground together in an agate mortar and then compressed into a pellet of 9.64-mm diameter with a pressure of 4000 kg/cm^2.

The experimental arrangement is depicted in Fig. 2. The fused silica tube is connected by appropriate valves to a tank of O_2 or vacuum or atmosphere. The tube is surrounded by two coaxial furnaces. The brass core of the inner one reaches to within about 2 cm of the end of the fused silica tube. The resistance heating coil is restricted to the lower end of the brass tube. The outer furnace is a resistance-type tube furnace. To prevent temperature fluctuation because of drafts, the major part of the apparatus shown in Fig. 2 is put into a box with a glass door.

In practice, the pellet is put into the fused silica tube; the tube is evacuated, then filled

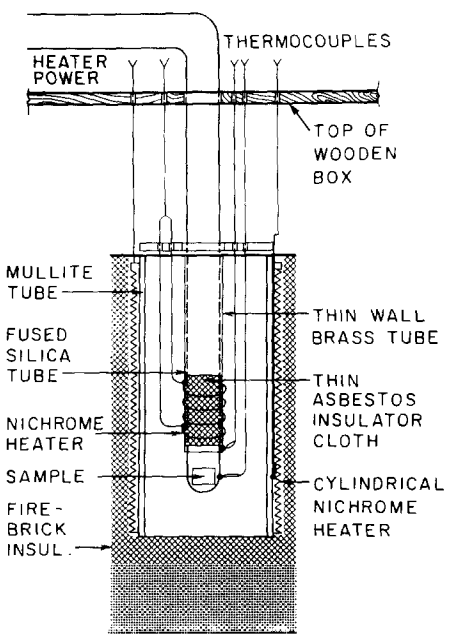

FIG. 2. Apparatus for the preparation of $Ag_{26}I_{18}W_4O_{16}$ by solid state reaction.

with O_2; this process is repeated once or twice. The O_2 pressure is controlled by a diaphragm valve. Temperatures are adjusted so that the inner furnace gives 330°C above the pellet and the outer furnace gives 280°C in the vicinity of the pellet. The 330°C temperature above the specimen prevents the evaporation of the AgI from the pellet.

In our case, the pellet was first heated in O_2 at a pressure of 3.5 atm for 6 hr. The tube was removed from the furnace and cooled. The pellet was removed and crushed, the material reground in an agate mortar, repelletized, and reinserted into the tube. The tube was evacuated, filled with O_2 to a pressure of 7 atm, and heated at the same temperature as before for 23 hr. The tube was removed, cooled, and the pellet removed. A powder X-ray diffraction photograph showed the material to be single phase, and this conclusion was confirmed by the conductivity measurements.

The conductivity measurements were made in a way slightly different from those made on $Py_5Ag_{18}I_{23}$ (*6*). Instead of using silver electrodes with mercury amalgamated surfaces, we used silver-tipped copper electrodes, and instead of using these electrodes to contact the sample directly, we incorporated electrodes made up of equal weights of 1 μm Ag powder and the material itself onto the specimen to be measured. That is to say, first this electrode material (0.260 g) was put into the cylinder of the pill press and smoothed with the piston. On top of this was added 1.045 g of the material itself, again smoothed with the piston, and then again 0.260 g of the electrode material. This was compressed at a pressure of 4000 kg/cm^2. An amount of material equal to that of the pure material in the sandwich was compressed at the same pressure to determine the length of the specimen; it was 2.165 mm. Also, the pellet had a density of 6.49 g/cm^3. As is shown later, this is about 4% lower than the X-ray density.

For other details on the equipment and technique used, the reader is referred to the paper on $Py_5Ag_{18}I_{23}$ (*6*).

Results

A plot of log specific conductivity multiplied by the absolute temperature (σT) vs the reciprocal temperature is given in Fig. 3. At 25°C the measured *average* conductivity is 0.059 $(\Omega\ \text{cm})^{-1}$, factors of 1.25 and 1.5 higher than the values reported by Takahashi *et al.* (*11*) and by Shahi and Chandra (*16*), respectively. The lower values obtained by these authors (*11*, *16*) may be attributed to their not having materials of correct composition.

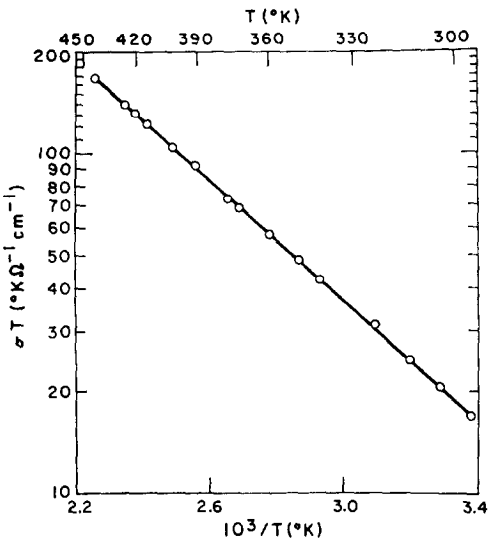

FIG. 3. Conductivity multiplied by absolute temperature versus reciprocal temperature.

The slope of the log σT vs $1/T$ plot (Fig. 3) gives an average Ag^+ ion activation enthalpy of motion of 4.1 kcal/mole or 0.18 eV.

Crystal Structure

Experimental

Crystals of the size sufficient for X-ray diffraction work were rather readily obtained by melting mixtures of 4.0–4.4 AgI to 1 "Ag_2WO_4" and then cooling. Initially, X-ray photographs taken with Buerger precession and Weissenberg cameras showed that crystals of $Ag_{26}I_{18}W_4O_{16}$ have diffraction symmetry $2/m$ and according to the conventional choice of axis are *C*-face centered. No other systematically absent reflections occur, implying that the crystal belongs to one of the following space groups (*17*): $C2/m$ (C_{2h}^3), Cm (C_s^3) or $C2$ (C_2^3).

A crystal was ground to a sphere of 0.105-mm radius with a sphere grinder (*18*) similar

to that described by Schuyff and Hulscher (*19*). (Both are modifications of the original Bond sphere grinder (*20*).) The crystal was aligned along the monoclinic *b*-axis. Initial lattice constants were determined from the precession camera photographs and refined after mounting on the single-crystal diffractometer. Final values were $a = 16.76 \pm 0.03$, $b = 15.52 \pm 0.03$, $c = 11.81 \pm 0.02$ Å, $\beta = 103.9 \pm 0.3°$. The unit cell contains 2 $Ag_{26}I_{18}W_4O_{16}$; the formula weight is 6080.28; the cell volume is 2982 Å^3. These give an X-ray density of 6.77 g/cm^3. The density of the carefully prepared polycrystalline specimen (see above), measured pycnometrically, is 6.72 g/cm^3, in good agreement with the X-ray density.

The intensity data were collected with a Buerger–Supper diffractometer automated by a Nova 1200 computer. Ag$K\alpha$ radiation and balanced Pd and Mo filters were used. The data collected were those of independent reflections in the range of $10° \leqslant 2\theta \leqslant 40°$. Each reciprocal lattice point was scanned at the rate of 1°/min over the range (1.5 + 0.5 Lp) where Lp is the Lorentz–polarization–Tunell factor. Background counts were taken at the beginning and at the end of the scan interval at one-sixth scan time of each scan. Intensities of data beyond $2\theta = 40°$ were not significant. Within the range $10° \leqslant 2\theta \leqslant 40°$, 2929 independent reflections were measured; of these 987 were below the 320-count threshold.

The Nova computer does some of the data processing, applying the background, absorption, and Lorentz–polarization–Tunell corrections and giving, on paper tape, the relative squares of the structure amplitudes. The *net* relative squares of the structure amplitudes are obtained by processing the data taken with the Pd and Mo filters with the CDC 6400 computer.

The linear absorption coefficient, μ, of $Ag_{26}I_{18}W_4O_{16}$ for Ag$K\alpha$ radiation is 144.55 cm^{-1}; from which, for $R = 0.105$ mm, $\mu R = 1.52$.

Determination and Refinement of the Structure

It was expected that the crystal structure would contain tetratungstate, $(W_4O_{16})^{8-}$ ions similar to those found in $Ag_8W_4O_{16}$ (*13*). In the latter, the symmetry of the $(W_4O_{16})^{8-}$ is simply 2. It was thought that the twofold axis of this ion would be coincident with the twofold axis of the crystal. If the symmetry of these ions remained just 2, then because the basis contains only a single $(W_4O_{16})^{8-}$ ion, it was to be expected that the most probable space group would be $C2$. However, although the symmetry of the $(W_4O_{16})^{8-}$ ion is 2, it is close to $2/m$, and if this ion controls the symmetry of the crystal, then it should also be expected that the symmetry of the crystal itself would be close to $2/m$. That is, pseudosymmetry was expected to characterize the crystal structure.

A three-dimensional Patterson map was calculated. As expected, this map was complicated by overlapping of many interatomic vectors between crystallographically nonequivalent ions. As in the cases of the other AgI-based solid electrolytes, it was expected that the structure would contain anion polyhedra which would share faces in such a manner as to form a network of pathways through which the Ag^+ ions could move. However, unlike the case of cation substitution, it was not known what role the oxygen atoms of the tetratungstate ions would play. (As will be seen later, it turns out to be a rather complicated one.)

After some trial structure calculations and model building, a promising trial structure with the $(W_4O_{16})^{8-}$ ions lying on the twofold axis was found. A calculation (*21*) of the structure amplitudes, including only the iodide ions and tungsten atoms for this model, gave an R, $\sum||F_o|-|F_c||/\sum|F_o|$, value of 42%. Several cycles of least-squares calculations (*21*) with isotropic thermal parameters brought the R-value down to 31%. The trial structure contained 90 iodide polyhedra, 88 tetrahedra, and 2 octahedra, per unit cell, with the type of connexity mentioned earlier.

Because of the *relatively* low conductivity for such a large number of Ag^+ ions per formula unit, it had been expected that some of the Ag^+ ions would have fixed positions, and that these should be located near the oxygen atoms of the $(W_4O_{16})^{8-}$ ions. The Ag^+ ions in the conduction channels were expected to be mobile, and therefore the individual polyhedral sites to have only an average partial occupancy.

A difference map revealed the positions of the eight crystallographically independent oxygen atoms of the $(W_4O_{16})^{8-}$ ion and of some of the Ag^+ ions—especially those positions involving both oxygen and iodide coordination, that were substantially occupied by Ag^+ ions. Trial values of occupancies of both types of sites were included in subsequent least-squares calculations.

Least-squares calculations, with anisotropic thermal parameters for all tungsten atoms and iodide ions and for some of the Ag^+ ions, were made with the NUCLS8 program (*22*) on the CDC 7600 computer at the Lawrence Berkeley Laboratory of the University of California. The final R-value is 9.2% for 1802 observed structure amplitudes; 140 were omitted because of interference by "dirty" radiation streaks.

Considering all possible positional, thermal, and occupancy parameters, the total comes to 646. This means that in a least-squares calculation, to refine all the parameters simultaneously a 646 × 646 component matrix would be inverted. We have varied at most 320 parameters in a single iteration. There are several reasons for this: (1) The structure has a pseudo-mirror plane giving, in some cases, very large parameter correlation coefficients (*23*), several being as high as 0.88. Because of the continued large oscillations, occupancy parameters related by the pseudocenter were constrained to be equal even though they cannot be truly so. (2) The (light) oxygen atom positional parameters could not be refined, and we took what appeared to be the best values for them that were obtained from repeated difference map calculations. (3) The positional parameters of sites that had a low Ag^+ ion occupancy could not be refined, and in these cases we again took what appeared to be the best values for them. (4) The oxygen atoms and the sites with low Ag^+ ion occupancy were assigned isotropic temperature factors which were held constant.

Calculations were also made to determine the correct enantiomorph. In two calculations, the one given herein (Table I) gave a *slightly* better R-value, 1–2%, than the other, based on the 1802 observed structure amplitudes. The $(W_4O_{16})^{8-}$ ion in the crystal on which the diffraction data were taken is the enantiomorph of the one in the $Ag_8W_4O_{16}$ crystal investigated (*13*).

In the calculations, the atomic scattering factors for Ag^+, W, and I^- were those of Cromer and Waber (*24*); for oxygen, those given by Tokonami (*25*) were used. Corrections for the real and imaginary parts of the anomalous dispersion were those given by Cromer (*26*). The observed data were weighted according to

$$\sigma = 0.036\,(F - 8) + 12.0 \qquad \text{for } F < 100,$$

$$\sigma = 16 \exp(-277/F) + 0.036\,(F - 8) + 12.0 \qquad \text{for } F \geqslant 100,$$

and $w = 1/\sigma^2$.

Of the 987 unobserved structure amplitudes only 26 calculated above the threshold values; these do not alter significantly the final value of the discrepancy factor, 9.2%. The standard error of an observation of unit weight is 1.01.

A table listing the observed and calculated structure amplitudes is available.[1] Table I lists the final positional and thermal parameters and multipliers (multiplier = one-half the number of atoms in a particular set of positions). Table II lists the interionic distances other than those of the tetratungstate ion itself, which are given in Fig. 2. Table III lists the following information regarding the anion polyhedra: First column, Ag^+ ion site designation; second, fractional occupancy of the site; third, number of apices in the polyhedron; fourth, average I–I distance in the polyhedron; fifth, average I–O distance in the polyhedron; sixth, average O–O distance; seventh, average Ag–I distance; eighth, average Ag–O distance; ninth, volume of the polyhedron; tenth, type of polyhedron (see below). Table IV gives the numbers of iodide and oxygen neighbors for each iodide and the average I–I and I–O distances for each iodide.

[1] See NAPS document No. 03063 for 12 pages of supplementary material. Order from ASIS/NAPS, Microfiche Publications, 440 Park Avenue South, New York, N.Y. 10016. Remit in advance $3.00 for microfiche copy or for photocopy, $5.00 up to 20 pages plus 25¢ for each additional page. All orders must be prepaid. Foreign orders add $3.00 for postage and handling.

TABLE I

FINAL VALUES OF ATOMIC PARAMETERS

ATOM		MULTIPLIER	X	Y	Z
W1		2.00	0.0748(2)	0	0.2390(3)
W2		1.00	0	0.1133	0
W3		1.00	0	-0.1067(4)	0
I1		2.00	0.0425(5)	0.6343(5)	0.1962(5)
I2		2.00	0.0390(5)	0.3746(7)	0.1945(11)
I3		2.00	0.1896(3)	0.5035(6)	-0.0099(5)
I4		2.00	0.3029(8)	0.2678(7)	0.1760(10)
I5		2.00	0.2983(6)	0.7299(8)	0.1696(8)
I6		2.00	0.2983(5)	0.5011(8)	0.3456(5)
I7		1.00	0	0.7658(10)	0.5000
I8		1.00	0	0.2398(10)	0.5000
I9		2.00	0.2559(9)	0.2421(7)	0.4972(11)
I10		2.00	0.3773(4)	0.0061(9)	0.4058(6)
O1	B	2.00	-0.015	0.094	0.148
O2	B	2.00	-0.020	-0.084	0.148
O3	B	2.00	0.091	0.182	0.040
O4	B	2.00	0.084	-0.184	0.051
O5	B	2.00	0.033	0.010	0.358
O6	B	2.00	0.078	-0.001	0.058
O7	B	2.00	0.133	0.089	0.256
O8	B	2.00	0.139	-0.095	0.260
A1	B	0.14(4))	0.500	0.000	0
A2	B	0.17(4))	0.350	0.000	0.805
A3	B	0.04(4))	0.300	-0.089	0.815
A3*	B	0.04	0.298	0.105	0.824
A4	B	0.23(4))	0.295	0.850	0.695
A4*	B	0.23	0.295	-0.850	0.695
A5	B	0.15(4))	0.352	0.340	0.386
A5*	B	0.15	0.354	0.665	0.383
A6	B	0.39(3)	0.335	0.182	0.382
A6*	B	0.39	0.352	0.820	0.390
A7	B	0.18(4))	0.602	0.155	0.435
A7*	B	0.18	0.607	-0.151	0.443
A8	B	0.24(4))	0.677	0.096	0.405
A8*	B	0.24	0.679	-0.094	0.408
A9		1.33(6)	0.625(2)	0.001(4)	0.359(3)
A10		0.96(5)	0.541(3)	0.020(3)	0.370(3)
A11	B	0.17(4))	0.510	-0.094	0.424
A11*	B	0.17	0.511	0.103	0.420
A12	B	0.04(4))	0.420	-0.159	0.310
A12*	B	0.04	0.427	0.159	0.313
A13	B	0.12(4))	0.378	-0.095	0.206
A13*	B	0.12	0.384	0.091	0.214
A14	B	0.08(4))	0.432	0.005	0.205
AO1		2.00(3)	0.354(1)	0.498(2)	0.127(1)
AO2		1.32(3)	0.283(1)	0.397(2)	0.882(3)
AO2*		1.32	0.280(2)	0.608(2)	0.879(4)
AO3	U	0.00	0.278	0.500	0.570
AO4	B	0.22(3)	0.268	0.135	0.318
AO4*	B	0.22	0.268	-0.135	0.318
AO5		1.40(3)	0.371(2)	-0.265(1)	0.727(2)
AO5*		1.40	0.344(1)	0.264(1)	0.796(2)
AO6		0.71(4)	0.270(4))	0.570(3))	0.543(3))
AO6*		0.71	0.266(3))	0.416(3))	0.548(4))
AO7	B	0.37(3)	0.368	-0.377	0.514
AO7*	B	0.37	0.368	0.378	0.515
AO8	B	0.08(4))	0.405	0.279	0.665
AO8*	B	0.08	0.410	0.715	0.660
AO9		0.51(3)	0.447	0.566(5)	0.460
AO9*		0.51	0.446(4))	0.443	0.460(5))
AO10		0.51(4))	0.421	0.379	0.311
AO10*		0.51	0.417(3))	-0.366(4))	0.307(4))
AO11		0.49(3)	0.224	0.423	0.782
AO11*		0.49	0.221	-0.421	0.780
AO12		1.49(4))	0.467(2)	0.301(2)	0.265(2)
AO12*		1.49	0.475(2)	-0.287(2)	0.263(2)
AO13	U	0.00	0.460	0.315	0.715
AO13*	U	0.00	0.460	0.693	0.710
AO14		2.00(3))	0.393(2)	0.182(2)	0.023(2)
AO14*		2.00	0.378(2)	0.828(1)	-0.006(2)
AO15	U	0.00	0.350	0.575	0.148
AO15*	U	0.00	0.350	0.438	0.149
AO16	U	0.00	0.330	0.390	0.020
AO16*	U	0.00	0.330	0.610	0.030

ANISOTROPIC THERMAL PARAMETERS(X10⁴)

ATOM	B11	B22	B33	B12	B13	B23
W1	26(2)	51(2)	44(2)	2(2)	-5(2)	10(3)
W2	12(2)	25(2)	46(4)	0	9(3)	0
W3	57(4)	50(4)	34(5)	0	-1(4)	0
I1	49(4)	38(3)	18(4)	0(3)	7(3)	-12(3)
I2	32(3)	61(5)	197(13)	8(4)	28(5)	-19(6)
I3	30(2)	48(3)	74(4)	14(4)	11(3)	13(5)
I4	52(5)	76(5)	83(9)	-93(4)	12(6)	3(5)
I5	31(3)	69(4)	63(7)	17(3)	-2(4)	12(4)
I6	68(4)	80(4)	74(5)	-31(5)	25(4)	-9(6)
I7	81(10)	78(8)	85(10)	0	-7(7))	0
I8	46(6)	88(7)	51(5))	0	12(4)	0
I9	61(4)	75(5)	85(6)	23(4)	-6(4)	-19(5)
I10	45(3)	78(4)	116(6)	-10(5)	11(4)	75(7)
A9	113(20))	272(43))	263(48))	93(32))	21(25))	147(47))
A10	216(40))	169(31))	185(16))	121(20))	136(20))	149(25))
AO1	25(3)	214(12)	120(9)	17(9)	18(4)	13(16)
AO2	29(6))	88(10))	335(39))	-18(7))	86(13))	-85(17))
AO2*	78(13))	78(12))	407(57))	37(10))	109(23))	63(22))
AO5	168(18))	48(6))	151(20))	-70(10))	-99(16))	50(10))
AO5*	28(5))	72(8))	122(15))	-1(5))	0(7))	7(8))
AO6	84(15))	96(17))	179(32))	-25(12))	70(20))	-56(20))
AO6*	103(16))	136(18))	67(31))	18(13))	-68(21))	-34(19))
AO9	212(48))	179(24))	26(20))	-154(23))	13(18))	8(8))
AO9*	93(25))	95(25))	113(42))	50(18))	58(28))	24(20))
AO10	189(48))	75(33))	245(93))	-48(32))	184(57))	-96(42))
AO10*	27(15))	85(38))	117(34))	26(20))	-35(20))	-64(30))
AO11	80(27))	16(28))	270(50))	-25(22))	90(35))	-14(32))
AO11*	26(26))	215(28))	164(49))	16(22))	30(35))	100(33))
AO12	93(11)	162(15)	48(11)	-51(10)	10(9)	37(10)
AO12*	65(9)	79(9)	179(23)	-33(7)	16(11)	-65(12)
AO14	101(9)	96(9)	173(17)	2(8)	22(10)	4(10)
AO14*	139(12)	47(5)	179(16)	37(6)	117(12)	19(6)

Note. B indicates isotropic thermal parameter held constant at 6.9 Å², U indicates site unfavorable to occupancy by Ag^+ ion,)) indicates standard error from a previous LS cycle in which the parameter was last varied.

TABLE II

INTERATOMIC DISTANCES AND STANDARD ERRORS

DESIG-NATION	DISTANCE (Å)	DESIG-NATION	DISTANCE (Å)	DESIG-NATION	DISTANCE (Å)	DESIG-NATION	DISTANCE (Å)	DESIG-NATION	DISTANCE (Å)	DESIG-NATION	DISTANCE (Å)
I9I1	4.63(3)	I315"	4.67(2)	I608	4.75	A5•I6	2.71	A11•I1	2.86	AO4O7	2.24
I9I2	4.90(3)	I316	4.17(2)	I702(2)	4.71	A5•I8	2.76	A11•I7	2.72	AO4I4	2.80
I9I4	4.07(2)	I4I5	4.08(2)	I705(2)	4.23	A5•I9	2.84	A11•I10	2.67	AO4I9	2.74
I9I5	4.26(2)	I4I6	4.15(2)	I708(2)	4.60	A6I4	2.74	A11•I10"	2.86	AO4I10	2.74
I9I6	4.52(2)	I4I7(2)	4.41(3)	I801(2)	4.69	A6I7	2.69	A12I2	2.72	AO4•O8	2.21
I9I6"	4.36(2)	I5I8	4.12(2)	I805(2)	4.04	A6I9	2.69	A12I5	2.87	AO4•I5	2.86
I9I7(2)	4.10(2)	I5I8(2)	4.50(3)	I807(2)	4.73	A6I10	2.75	A12I8	2.80	AO4•I9	3.00
I9I8(2)	4.30(2)	I6I7(2)	5.01(2)	I907	3.87	A6•I5	2.90	A12I10	2.96	AO4•I10	2.88
I9I10	4.45(2)	I6I8(2)	5.05(2)	I908	3.92	A6•I8	2.80	A12•I1	2.66	AO5O3	2.80
I9I10"	4.93(2)	O5O5'	3.78	I1007	4.18	A6•I9	2.77	A12•I4	2.86	AO5O7	2.28
I10I1	4.59(2)	I102	4.50	I1008	4.27	A6•I10	2.92	A12•I7	2.80	AO5I2	2.68(2)
I10I1'	4.98(2)	I104	3.46	A1I1(2)	3.07	A7I1	2.78	A12•I10	2.82	AO5I4	3.41(4)
I10I2	4.58(2)	I104'	4.24	A1I2(2)	2.96	A7I7	2.66	A13I2	2.78	AO5I9	2.97(3)
I10I2'	5.02(2)	I108	4.50	A1I3(2)	3.21	A7I9	2.69	A13I3	2.78	AO5•O4	2.64
I10I3	4.54(2)	I201	4.46	A2I1	2.76	A7I10	2.95	A13I5	3.01	AO5•O8	2.21
I10I4	4.91(2)	I203	3.71	A2I2	2.69	A7•I2	2.91	A13I10	2.84	AO5•I1	2.75(2)
I10I5	5.11(2)	I203'	4.30	A2I3	2.66	A7•I8	2.67	A13•I1	2.80	AO5•I5	2.92(2)
I10I6	4.62(3)	I207	4.73	A2I6	2.69	A7•I9	2.94	A13•I3	2.78	AO5•I9	2.87(3)
I10I7(2)	4.54(2)	I301	5.05	A3I2	2.79	A7•I10	3.00	A13•I4	3.05	AO6O7	2.52
I10I8(2)	4.63(2)	I302	4.97	A3I3	2.68	A8I1	2.97	A13•I10	2.65	AO6I6	2.70(6)
I10I10'	4.18(3)	I303	4.69	A3I4	2.83	A8I6	2.73	A14I1	2.75	AO6I9	2.73(6)
I1I1'	4.51(2)	I304	5.27	A3I6	2.61	A8I9	2.67	A14I2	2.73	AO6I10	2.86(6)
I1I2	4.03(1)	I304"	4.90	A3•I1	2.78	A8I10	2.96	A14I3	2.69	AO6•O8	2.45
I1I3	4.36(2)	I306	4.07	A3•I3	2.67	A8•I2	3.04	A14I10	2.74	AO6•I6	2.88(4)
I1I3'	4.47(2)	I307	4.75	A3•I5	2.54	A8•I6	2.72	AO1O1	2.62	AO6•I9	2.76(6)
I1I4	4.48(2)	I308	4.85	A3•I6	2.78	A8•I9	2.93	AO1O2	2.43	AO6•I10	2.94(4)
I1I5	4.63(2)	I402	3.83	A4I2	2.80	A8•I10	3.02	AO1O6	2.70	AO7O5	2.63
I1I6	4.71(2)	I403	3.77	A4I4	2.80	A9I1	2.93(4)	AO1I3	2.84(2)	AO7O7	2.79
I1I7(2)	4.33(1)	I404	3.72	A4I6	2.80	A9I2	2.89(6)	AO1I6	2.96(2)	AO7I6	2.78
I2I2'	4.46(3)	I407	4.18	A4I9	2.79	A9I6	2.94(4)	AO2O4	2.52	AO7I8	2.90
I2I3	4.37(2)	I501	3.82	A4•I1	2.73	A9I10	2.79(4)	AO2O6	2.76	AO7I9	2.76
I2I3'	4.41(3)	I503	3.50	A4•I5	2.79	A10I1	2.72(3)	AO2O8	2.38	AO7•O5	2.83
I2I4	4.78(2)	I504	3.78	A4•I6	2.77	A10I2	3.06(5)	AO2I3	2.79(2)	AO7•O8	2.72
I2I5	4.56(2)	I508	4.15	A4•I9	2.68	A10I10	2.88(5)	AO2I5	2.93(2)	AO7•I6	2.80
I2I6	4.71(2)	I601	4.57	A5I4	2.66	A10I10"	2.68(4)	AO2•O3	2.43	AO7•I7	2.85
I2I8(2)	4.35(2)	I602	4.47	A5I6	2.66	A11I2	2.91	AO2•O6	2.87	AO7•I9	2.80
I3I4	4.45(2)	I605	3.91	A5I7	2.77	A11I8	2.75	AO2•O7	2.36	AO8O8	2.33
I3I4"	4.57(2)	I605'	3.93	A5I9	2.77	A11I10	2.68	AO2•I3	2.76(3)	AO8I1	2.80
I3I5	4.28(2)	I607	4.76	A5•I5	2.67	A11I10"	2.86	AO2•I4	2.84(3)	AO8I7	2.80

Note. Designation example: *A*O6O7 means the distance between the site *A*O6 and the oxygen atom O7. See text for meanings of *, ′, ″. (2) following a designation means two equal distances caused by a twofold axis.

TABLE II—*Continued*

DESIG-NATION	DISTANCE (Å)	DESIG-NATION	DISTANCE (Å)	DESIG-NATION	DISTANCE (Å)	DESIG-NATION	DISTANCE (Å)	DESIG-NATION	DISTANCE (Å)	DESIG-NATION	DISTANCE (Å)
AO8I9	2.85	AO1404	2.32	A5•A6•	2.41	A11•A7	1.70	AO5•A4•	1.96	AO10•AO9	2.05
AO8•O7	2.42	AO14I1	2.92(3)	A5•AO7	1.64	A11•A10	1.55	AO5•AO4•	2.41	AO10•AO12•	1.72
AO8•I2	3.02	AO14I1'	3.13(3)	A5•AO10•	1.62	A11•A11•	2.01	AO5•AO8	1.49	AO11A13	1.77
AO8•I8	2.71	AO14I3	3.08(2)	A6A5	2.46	A11•A12•	1.87	AO6A8	2.01	AO11AO2	1.41
AO8•I9	2.98	AO14I4	2.94(3)	A6A7	2.14	A12A6•	1.68	AO6AO4	2.15	AO11AO4•	1.52
AO9O5	2.26	AO14I5	3.54(3)	A6AO4	1.78	A12A11	2.03	AO6AO6•	2.39(6)	AO11•A13•	1.79
AO9O5'	2.27	AO14•O3	2.38	A6A12•	1.51	A12A13	1.61	AO6AO7	1.94	AO11•AO2•	1.41
AO9I6	2.72	AO14•I2	3.22(3)	A6•A5•	2.41	A12AO12•	2.31	AO6•A8•	1.93	AO11•AO4	1.49
AO9I8	2.84	AO14•I2'	2.98(2)	A6•A7•	1.98	A12•A6	1.51	AO6•AO4•	1.97	AO12A12•	2.41
AO9•O5	2.35	AO14•I3	2.97(2)	A6•AO4•	1.62	A12•A11•	1.87	AO6•AO6	2.39(6)	AO12AO8	2.13
AO9•O5'	2.34	AO14•I4	3.34(3)	A6•A12	1.68	A12•A13•	1.61	AO6•AO7•	1.93	AO12AO10	1.60
AO9•I6	2.67	AO14•I5	3.11(2)	A7A6	2.14	A12•AO12	2.41	AO7A5•	1.64	AO12•A12	2.31
AO9•I7	2.90	A1A2(2)	2.97	A7A8	1.66	A13A12	1.61	AO7AO6	1.94	AO12•AO8•	1.92
AO1OO2	2.44	A1A14(2)	2.91	A7A11•	1.70	A13A14	1.80	AO7AO8•	2.22	AO12•AO10•	1.72
AO1OO5	2.73	A1AO14(2)	3.39	A7AO8	2.25	A13AO11	1.77	AO7AO9	1.83	AO14A1	3.39
AO1OI4	2.81	A1AO14•(2)	3.35	A7•A6•	1.98	A13•A12•	1.61	AO7•A5	1.60	AO14A3•	2.77
AO1OI6	2.90	A2A1	2.97	A7•A8•	1.63	A13•A14	1.58	AO7•AO6•	1.93	AO14A13•	2.70
AO1OI7	2.90	A2A3	1.64	A7•A11	1.82	A13•AO11•	1.79	AO7•AO8	2.31	AO14AO5•	3.53(3)
AO1O•O1	2.50	A2A3•	1.89	A7•AO8•	2.39	A14A1	2.91	AO7•AO9•	1.89	AO14•A1	3.35
AO1O•O5	2.70	A2A9	2.08	A8A4•	1.61	A14A10	2.34	AO8A7	2.25	AO14•A3	2.55
AO1O•I5	2.69(5)	A3A2	1.64	A8A7	1.66	A14A13	1.80	AO8AO5•	1.49	AO14•A13	2.77
AO1O•I6	2.98(7)	A3A4	1.69	A8A9	1.73	A14A13•	1.58	AO8AO7•	2.31	AO14•AO5	3.44(3)
AO1O•I8	2.88(5)	A3AO14•	2.55	A8AO6	2.01	AO1AO2	3.25(4)	AO8AO12	2.13	AO15A3•	2.62
AO11O8	2.50	A3•A2	1.89	A8•A4	1.64	AO1AO2•	3.36(5)	AO8•A7•	2.39		
AO11I3	2.94	A3•A4•	1.67	A8•A7•	1.63	AO1AO10	2.87	AO8•AO5	1.18		
AO11I5	3.09	A3•AO14	2.77	A8•A9	1.75	AO1AO10•	3.00	AO8•AO7	2.22		
AO11I10	2.77	A4A3	1.69	A8•AO6•	1.93	AO2AO11	1.41	AO8•AO12	1.92		
AO11•O7	2.50	A4A5	2.42	A9A2	2.08	AO2•AO11•	1.41	AO9AO7	1.83		
AO11•I3	2.90	A4A8•	1.64	A9A8	1.73	AO4A6	1.78	AO9AO9	1.80		
AO11•I4	3.02	A4AO5	2.17	A9A8•	1.75	AO4AO5	2.74	AO9AO9•	1.91		
AO11•I10	2.66	A4•A3•	1.67	A9A10	1.47(4)	AO4AO6	2.15	AO9AO10•	2.05		
AO12O2	2.30	A4•A5•	2.46	A10A9	1.47(4)	AO4AO11•	1.49	AO9•AO7•	1.89		
AO12I1	3.07(3)	A4•A8	1.61	A10A11	1.99	AO4•A8•	1.62	AO9•AO9	1.91		
AO12I4	2.74(3)	A4•AO5•	1.96	A10A11•	1.55	AO4•AO5•	2.41	AO9•AO9•	1.83		
AO12I7	2.75(2)	A5A4	2.42	A10A14	2.34	AO4•AO6•	1.97	AO9•AO10	1.98		
AO12•O1	2.32	A5A6	2.46	A11A7•	1.82	AO4•AO11	1.52	AO10A5	1.73		
AO12•I2	2.92(3)	A5AO7•	1.60	A11A10	1.99	AO5A4	2.17	AO10AO9•	1.98		
AO12•I5	2.90(3)	A5AO10	1.73	A11A11	1.90	AO5AO4	2.74	AO10AO12	1.60		
AO12•I8	2.76(2)	A5•A4•	2.46	A11A12	2.03	AO5AO8•	1.18	AO10•A5•	1.62		

TABLE III

POLYHEDRA FOR Ag^+ ION SITES

SITE	FRACTIONAL OCCUPANCY	NO. OF APICES	AVERAGE I-I DISTANCE(Å)	AVERAGE I-O DISTANCE(Å)	AVERAGE O-O DISTANCE(Å)	AVERAGE AG-I DISTANCE(Å)	AVERAGE AG-O DISTANCE(Å)	VOLUME(Å^3)	TYPE
A1	0.140	6	(12) 4.35	-	-	(6) 3.13	-	38.5	C
A2	0.085	4	(6) 4.39	-	-	(4) 2.70	-	9.7	C
A3	0.020	4	(6) 4.44	-	-	(4) 2.73	-	10.1	C
A3*	0.020	4	(6) 4.39	-	-	(4) 2.69	-	9.7	C
A4	0.115	4	(6) 4.52	-	-	(4) 2.80	-	10.6	C
A4*	0.115	4	(6) 4.45	-	-	(4) 2.74	-	10.3	C
A5	0.075	4	(6) 4.38	-	-	(4) 2.72	-	9.5	C
A5*	0.075	4	(6) 4.43	-	-	(4) 2.75	-	9.9	C
A6	0.195	4	(6) 4.42	-	-	(4) 2.72	-	9.9	C
A6*	0.195	4	(6) 4.62	-	-	(4) 2.85	-	11.4	C
A7	0.090	4	(6) 4.51	-	-	(4) 2.77	-	10.5	C
A7*	0.090	4	(6) 4.64	-	-	(4) 2.88	-	11.9	C
A8	0.120	4	(6) 4.62	-	-	(4) 2.83	-	11.6	C
A8*	0.120	4	(6) 4.78	-	-	(4) 2.93	-	12.8	C
A9	0.665	4	(6) 4.68	-	-	(4) 2.89	-	11.7	C
A10	0.480	4	(6) 4.56	-	-	(4) 2.84	-	10.6	C
A11	0.085	4	(6) 4.57	-	-	(4) 2.80	-	10.9	C
A11*	0.085	4	(6) 4.53	-	-	(4) 2.78	-	10.7	C
A12	0.020	4	(6) 4.55	-	-	(4) 2.84	-	11.5	C
A12*	0.020	4	(6) 4.54	-	-	(4) 2.79	-	10.9	C
A13	0.080	4	(6) 4.58	-	-	(4) 2.85	-	11.7	C
A13*	0.080	4	(6) 4.59	-	-	(4) 2.82	-	11.3	C
A14	0.040	4	(6) 4.51	-	-	(4) 2.73	-	10.2	C
AO1	1.000	5	(1) 4.17	(5) 4.62	(3) 2.77	(2) 2.90	(3) 2.58	12.2	F
AO2	0.660	5	(1) 4.67	(5) 4.35	(3) 2.80	(2) 2.86	(3) 2.55	11.9	B
AO2*	0.660	5	(1) 4.57	(5) 4.29	(3) 2.81	(2) 2.80	(3) 2.55	11.9	B
AO4	0.110	4	(3) 4.46	(5) 4.08	-	(3) 2.76	(1) 2.24	8.9	C
AO4*	0.110	4	(3) 4.77	(5) 4.11	-	(3) 2.91	(1) 2.21	9.8	C
AO5	0.700	5	(3) 4.58	(5) 4.05	(1) 2.87	(3) 3.02	(2) 2.54	16.2	B
AO5*	0.700	5	(3) 4.50	(5) 3.96	(1) 2.78	(3) 2.85	(2) 2.43	15.3	C
AO6	0.355	4	(3) 4.48	(3) 4.27	-	(3) 2.76	(1) 2.52	9.6	C
AO6*	0.355	4	(3) 4.48	(3) 4.31	-	(3) 2.86	(1) 2.45	10.2	C
AO7	0.185	5	(3) 4.57	(5) 4.27	(1) 2.66	(3) 2.81	(2) 2.71	17.3	C
AO7*	0.185	5	(3) 4.54	(5) 4.29	(1) 2.84	(3) 2.82	(2) 2.78	17.1	C
AO8	0.040	4	(3) 4.35	(5) 4.34	-	(3) 2.82	(1) 2.33	9.4	C
AO8*	0.040	4	(3) 4.52	(3) 4.44	-	(3) 2.90	(1) 2.42	10.0	C
AO9	0.255	4	(1) 5.05	(4) 3.98	(1) 3.97	(2) 2.78	(2) 2.27	7.7	C
AO9*	0.255	4	(1) 5.05	(4) 3.98	(1) 3.97	(2) 2.79	(2) 2.35	8.2	C
AO10	0.255	5	(3) 4.52	(5) 4.23	(1) 2.83	(3) 2.87	(2) 2.59	17.3	C
AO10*	0.255	5	(3) 4.56	(5) 4.20	(1) 2.48	(3) 2.85	(2) 2.60	17.1	C
AO11	0.245	4	(3) 4.78	(3) 4.42	-	(3) 2.93	(1) 2.50	10.8	C
AO11*	0.245	4	(3) 4.66	(3) 4.37	-	(3) 2.86	(1) 2.50	10.5	C
AO12	0.745	4	(3) 4.41	(3) 4.33	-	(3) 2.85	(1) 2.30	9.6	B
AO12*	0.745	4	(3) 4.47	(3) 4.32	-	(3) 2.86	(1) 2.32	9.7	B
AO14	1.000	6	(8) 4.44	(4) 3.80	-	(5) 3.12	(1) 2.32	32.2	F
AO14*	1.000	6	(8) 4.49	(4) 3.82	-	(5) 3.12	(1) 2.38	33.4	F

Notes. 1. Number in parentheses is the number of distances in the average. 2. Under "Type," C designates site in conduction passageway, B designates bypass site, F designates filled site.

TABLE IV

COORDINATIONS OF THE I^- IONS AND AVERAGE DISTANCES IN ANGSTROMS

Iodide designation	No. of I^- neighbors	Average I–I distance	No. of O^{2-} neighbors	Average I–O distance
I1	11	4.52(2)	4	4.18
I2	11	4.56(2)	4	4.30
I3	10	4.43(2)	8	4.82
I4	9	4.43(2)	4	3.88
I5	9	4.47(2)	4	3.81
I6	10	4.54(2)	6	4.40
I7	10	4.48(2)	6	4.51
I8	10	4.57(2)	6	4.49
I9	10	4.45(2)	2	3.90
I10	13	4.70(2)	2	4.23

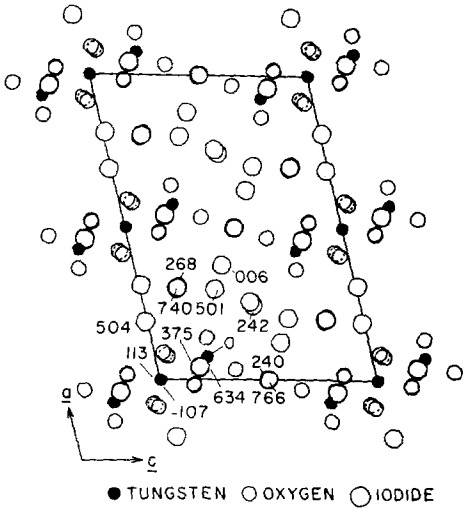

FIG. 4. [010] projection of the structure of $Ag_{26}I_{18}W_4O_{16}$. Ag^+ ion positions are excluded. The y values ($\times 10^3$) of the I^- ions and W atoms are indicated for the asymmetric unit.

Description of the Structure

A projection of the structure down the *b*-axis is shown in Fig. 4. There are three crystallographically independent tungsten atoms and 10 independent iodide ions (Table I) in the asymmetric unit of the structure. The $(W_4O_{16})^{8-}$ ions lie on twofold axes, at the corners and *C*-face centers of the unit cell, and are well separated by the surrounding three-dimensional network of face-sharing iodide polyhedra through which the Ag^+ ions can move. All iodide polyhedra are in conduction passageways. The oxygen atoms associated with the $(W_4O_{16})^{8-}$ ions also form polyhedra with surrounding iodide ions (Fig. 5); most of these mixed I–O polyhedra are occupied, some fully, by Ag^+ ions (see Tables I and III). Some of the mixed I–O polyhedra are in conduction channels, some are not (see below).

The atoms I3, I6, I10, and W1, and their equivalents, lie approximately on the planes $y = 0, \frac{1}{2}$; I4, I5, I7, I8, and I9 and their equivalents lie approximately on the planes $y = \pm\frac{1}{4}$; I1, and W2 and their equivalents lie approximately on the planes $y = \frac{1}{8}, \frac{5}{8}$; and I2 and W3 and their equivalents lie approximately on the planes $y = \frac{3}{8}, \frac{7}{8}$. Thus the W atoms and I^- ions all lie in layers approximately $b/8$ apart (Fig. 4). The whole structure approximates to a centrosymmetric one, apparently dominated by the deviation from centrosymmetry of the $(W_4O_{16})^{8-}$ ion itself as in the case of $Ag_8W_4O_{16}$ (*13*). The pseudo-mirror planes are located at $y = 0, \frac{1}{2}$. The pseudosymmetric pairs are W2 and W3, I1 and I2, I4 and I5, I7 and I8, and pairs of I9. Similar pairing occurs for the oxygen atoms and for the Ag^+ ion sites. The iodide polyhedral sites are labeled A, mixed I–O sites, AO; those with * are pseudo-mirror related to those without * (see Table I).

We denote an equivalent atom obtained by

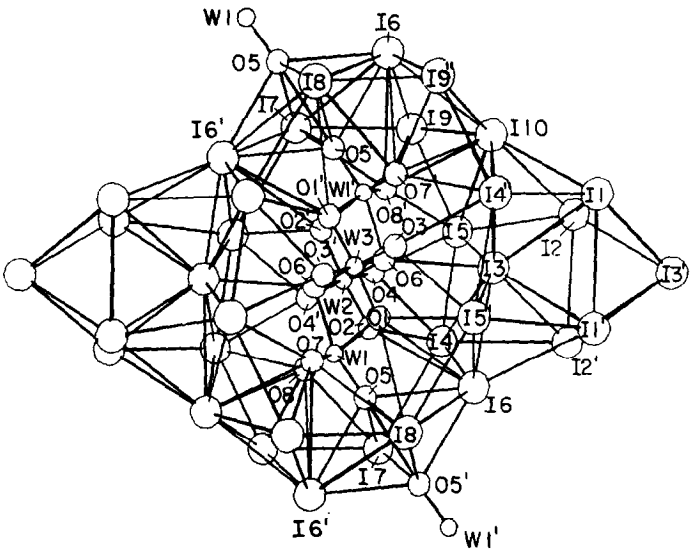

FIG. 5. The surroundings of the $(W_4O_{16})^{8-}$ ion looking down the *b*-axis (which passes through W2 and W3). The iodide octahedra above and below the $(W_4O_{16})^{8-}$ ion are omitted. Parts of neighboring $(W_4O_{16})^{8-}$ ions are included.

the operation of a twofold axis by a single prime and one obtained by the operation of a twofold screw axis by a double prime. There is one independent iodide octahedron (or two equivalent iodide octahedra) in the unit cell, formed by I1, I2, I3, and I1′, I2′, I3′. The centers of the octahedra are at 0, $\frac{1}{2}$, 0 and $\frac{1}{2}$, 0, 0. Four faces of a single octahedron share faces with mixed I–O octahedra (Fig. 6). The mixed I–O octahedra share only edges or corners with other mixed octahedra. Thus each block of five octahedra separates two pairs of $(W_4O_{16})^{8-}$ ions in the *a*- and *b*-directions (Fig. 6). The $(W_4O_{16})^{8-}$ ions, the blocks of octahedra, and the I–O polyhedra between the two, form a wall about (001) planes at $-0.2 < z < 0.2$ (Fig. 6). The mixed I–O octahedra, *A*O14 and *A*O14*, are fully occupied by Ag^+ ions, in contrast with the low fractional occupancy, 0.14, of the iodide octahedra (A1 in Table I). The I–O polyhedra *A*O1, *A*O2, *A*O2*, *A*O1′, *A*O2′, *A*O2*′ also have high occupancy (see Tables I and III); therefore conduction through the wall is most likely to occur via the A1 (octahedral) sites.

The network formed from the 88 iodide tetrahedra (22 independent tetrahedral sites, Table I) lies between the walls, i.e., in the region $0.2 < z < 0.8$ (see Fig. 4). A stereoscopic view of the complete iodide arrangement is shown in Fig. 7; atoms O7 and O8 (from the tetratungstate ions) are included because they are at two corners of an icosahedron, of which there are four per unit cell; atom O5 is included because it is part of the mixed I–O tetrahedra that are in conduction passageways. The icosahedra involve all the independent iodide ions except I2. There are thus 10 *iodide* tetrahedra per icosahedron; the sites are designated *A*4–*A*8 and *A*4*–*A*8*. The 10 mixed I–O tetrahedral sites are designated *A*O4–*A*O8, *A*O4*–*A*O8* (see Tables I and III).

In the [010] direction, the icosahedra are linked by the mixed I–O tetrahedra formed from I6, I10, O7, and O8 (site *A*O3 in Table II). In the [100] direction, the icosahedra share corners I7 and I8; the width of the icosahedron is the I9–I9′ distance, approximately *a*/2. The icosahedra are not directly linked to each other in the [001] direction; however, they are linked to iodide octahedra in the wall (see above) through iodide tetrahedra. The four faces of an iodide octahedron *not* shared with mixed I–O octahedra are shared with *connecting* iodide tetrahedra, two on each side of the wall. These connecting tetrahedra are

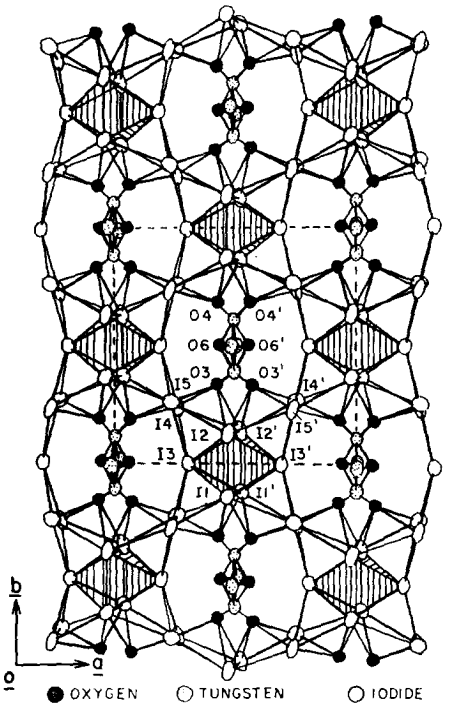

FIG. 6. The structure in the region $-0.2 < z < 0.2$ called the "wall" in the text. O3, O3′, O4, O4′ are involved in the formation of mixed I–O octahedra; O6 and O6′ are included to help show the orientation of the $(W_4O_{16})^{8-}$ ion. The other 10 oxygen atoms per $(W_4O_{16})^{8-}$ ion are not shown. For O–I connections other than those involved in the formation of the mixed I–O octahedra, see Fig. 5. The *pure* iodide octahedra are shaded.

not themselves in the icosahedra. One of these faces of the octahedron is I1, I2, I3, connecting it to one icosahedron via $A2 \rightarrow A3 \rightarrow A4$ and to another icosahedron via $A2 \rightarrow A3^* \rightarrow A4^*$. The symmetry equivalent octahedral face I1′ I2′, I3′ similarly connects the octahedron to two icosahedra on the other side of the wall. The remaining two equivalent faces I1′, I2, I3′ and I1′, I2′, I3, open to iodide tetrahedra which are part of an array of iodide ions that form a "wheel" composed of face-sharing iodide tetrahedra (Fig. 8).

The wheel has three hexagonal rims as shown in Figs. 8 and 9 and consists of 20 I^- ions forming 30 tetrahedra each. There are two such wheels per unit cell. All the crystallographically nonequivalent I^- ions are involved in each wheel. As indicated above, wheels in neighboring cells, in the [001] direction, are linked by the iodide octahedra (Fig 9). Each wheel shares I9 corners with four other wheels. The I9 corners are the centers of the icosahedra. Twelve of the 30 tetrahedra in each wheel belong to two neighboring icosahedra (6 in each). An I^- tetrahedron that involves any I9 belongs to the icosahedron; if an I^- tetrahedron involves any I10, it belongs to the wheel; if it involves both an I9 and an I10, it is in both the wheel and the icosahedron. If the I^- tetrahedron involves neither an I9 nor an I10, it is a connecting tetrahedron between the icosahedron and the iodide octa-

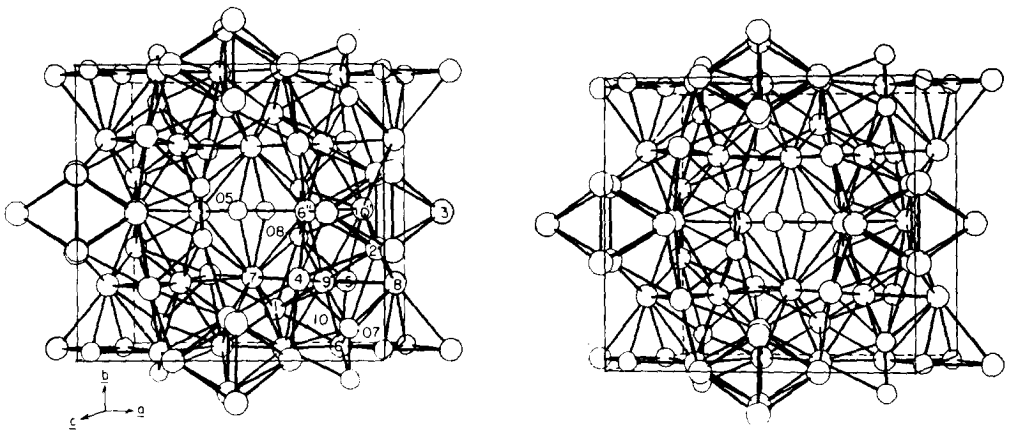

FIG. 7. Stereoscopic view down the *c*-axis. All iodides in the unit cell are shown, but only O5, O7, and O8 from the $(W_4O_{16})^{8-}$ ion are included. Atoms in the icosahedron have labels inside the circles; atoms not in the icosahedron have labels outside the circles. The four iodide octahedra are out front toward the viewer. The four icosahedra and the four mixed I–O tetrahedra formed from O5, O5′, I7, I8, I6, and I6′ are in the back.

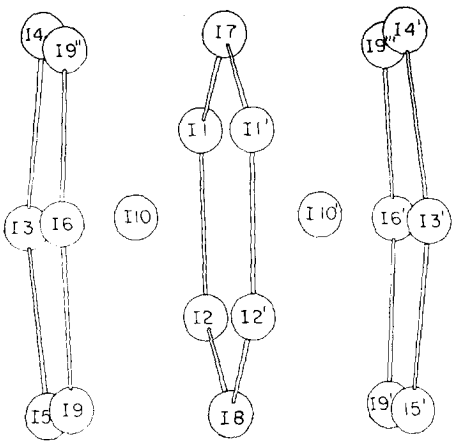

FIG. 8. The arrangement of iodide ions in a "wheel." Each such wheel contains 30 iodide tetrahedra.

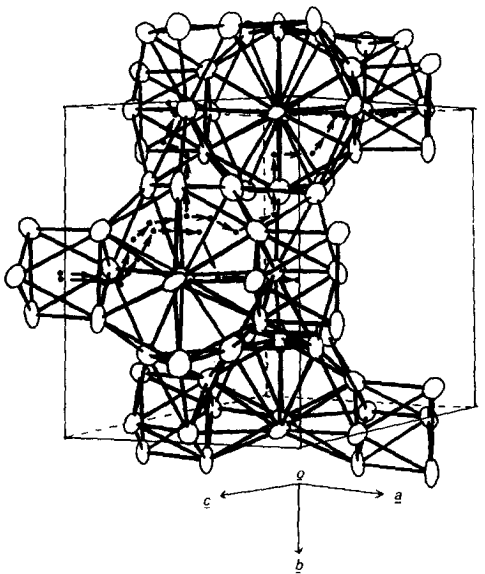

FIG. 9. Iodide arrangement looking down the wheel axis. One complete wheel is shown at the top. To show clearly a particular route in the [001] direction, only two spokes of the wheel at $y \approx \frac{1}{2}$ are included.

hedron. All but 12 of the 88 tetrahedra involve an I9 and/or an I10.

Surrounding *each* $(W_4O_{16})^{8-}$ ion, there are 60 polyhedra which are formed from both I^- ions and O atoms. Of the 120 I–O polyhedra in the unit cell, 8 are the filled octahedra which occur only in the wall region. The remaining 112 I–O polyhedra are either tetrahedra or five-cornered polyhedra. Of these, 28 are also in the wall region, and 16 (*A*O15, *A*O15*, *A*O16, *A*O16*) of these 28 are unoccupied because they are too close to the filled sites *A*O1. The fractional occupancy of the other 8, *A*O2 and *A*O2*, is 0.65, but the Ag^+ ions in these cannot go through the wall, because to do so, they must go into sites *A*O15, *A*O15*, *A*O16, *A*O16*, which is apparently forbidden. The Ag^+ ions could, however, leave the *A*O2 and *A*O2* sites on a single side of the wall by entering sites *A*O5 (*A*O5*) or *A*O11 (*A*O11*), the latter being in a conduction passageway; the *A*O5 (*A*O5*) may be called bypass sites (see below).

Thus far we have discussed 36 I–O polyhedra which are all in the wall region. Of the remaining 84 sites, namely *A*O3–*A*O13 and *A*O4*–*A*O13* (see Tables I and III), 12, *A*O3, *A*O13, and *A*O13*, are vacant because they are close, 2.92, 3.01, and 3.14 Å, respectively, to the W1 atom. Nevertheless, there is the remote possibility that Ag^+ ions do go through these. (In $Ag_8W_4O_{16}$ (*13*) the nearest Ag^+–W distance is 3.40 Å.) Of the 72 remaining sites, 16, *A*O5, *A*O5*, *A*O12, and *A*O12*, may be called bypass sites, like *A*O2 and *A*O2*, because they are not directly in conduction passageways. The remaining 56 sites, *A*O4, *A*O4*, *A*O6–*A*O11, *A*O6*–*A*O11*, are clearly in conduction passageways. This is actually consistent with their relatively low fractional occupancies, i.e., $f < 0.5$; the occupancies of the bypass sites are $0.5 < f < 1.0$.

The tilting of the $(W_4O_{16})^{8-}$ anions from the (100) plane (Fig. 4) causes the terminal oxygen atoms O5 to be at a distance of 3.78 Å from O5′ of the neighboring $(W_4O_{16})^{8-}$ ions (Fig. 5). Together with I6, I7, I8, the O5 and O5′ atoms form four tetrahedra, sites *A*O9, *A*O9*, *A*O9′, *A*O9*′. Sites *A*O10, *A*O10*, *A*O10′, *A*O10*′ share faces with these four connecting them with iodide tetrahedra. These mixed I–O sites are important, but they are not absolutely required for conduction in the *a*- and *b*-directions; that is, these sites permit more direct routes than just the pure iodide polyhedra alone.

Conduction Pathways

In the [001] direction, conduction is through the wheel-iodide octahedron-wheel-··· (Fig. 9).

One of the shortest routes is $A1 \rightarrow A14 \rightarrow A10 \rightarrow A11^* \rightarrow A10' \rightarrow A14' \rightarrow A1$. In the [010] direction, the Ag^+ ions can move (1) only in iodide tetrahedra or (2) in combinations of iodide tetrahedra and I–O polyhedra. An example of (1) is: Suppose there is an Ag^+ ion initially in an iodide tetrahedron belonging to a wheel centered at $(0, \frac{1}{2}, \frac{1}{2})$. It can move into the neighboring icosahedron in the [110] direction and then into the wheel centered at $(\frac{1}{2}, 1, \frac{1}{2})$. Because of the pseudosymmetry plane at $y = 0$, the Ag^+ ion can turn and move in the $[\bar{1}10]$ direction, first entering an icosahedron and then reaching the wheel centered at $(0, \frac{3}{2}, \frac{1}{2})$, i.e., one unit cell away from the initial wheel. In this manner, by moving first in the [110] and then in the $[\bar{1}10]$ direction, the Ag^+ ion has effectively traveled in the [010] direction. An example of (2) is: by utilizing mixed I–O polyhedra, one direct route is $AO9 \rightarrow AO9^* \rightarrow AO7^* \rightarrow AO8^* \rightarrow A7 \rightarrow A11^* \rightarrow A10 \rightarrow A11 \rightarrow A7^* \rightarrow AO8 \rightarrow AO7 \rightarrow AO9$ (in the next cell). An alternate route is $AO9 \rightarrow AO9^* \rightarrow AO10 \rightarrow A5 \rightarrow A6 \rightarrow A12^* \rightarrow A11^* \rightarrow A10 \rightarrow A11 \rightarrow A12 \rightarrow A6^* \rightarrow A5^* \rightarrow AO10^* \rightarrow AO9$ (in the next cell).

For conduction (effectively) in the [100] direction, an Ag^+ ion originally in a wheel centered at $(0, \frac{1}{2}, \frac{1}{2})$ can first move up the icosahedron in the [110] direction and then into the wheel centered at $(\frac{1}{2}, 1, \frac{1}{2})$ as described above. The Ag^+ ion can turn in the $[1\bar{1}0]$ instead of the $[\bar{1}10]$ direction, move through another icosahedron and reach the wheel centered at $(1, \frac{1}{2}, \frac{1}{2})$, a unit a from the initial wheel. In this manner only the iodide polyhedra would be involved. Again a more direct route involving also I–O polyhedra is $AO9 \rightarrow AO7 \rightarrow AO6 \rightarrow A8 \rightarrow A7 \rightarrow A12^* \rightarrow A11^* \rightarrow A12^{*\prime} \rightarrow A7' \rightarrow A6 \rightarrow AO4 \rightarrow AO6' \rightarrow AO7' \rightarrow AO9$ (in the next cell).

Discussion

In $Ag_{26}I_{18}W_4O_{16}$, the tetratungstate ion replaces eight iodide ions. The number of Ag^+ ions in the formula seems large relative to the number of iodide ions. The 90 iodide polyhedra by themselves cannot acccommodate the 52 Ag^+ ions in the unit cell. In fact, only a small proportion, 22.4% (Table V) of the Ag^+ ions are in these sites at room temperature. In the structure of $Ag_{26}I_{18}W_4O_{16}$, the oxygen atoms form polyhedra with the iodide ions. A large number, 56, of these polyhedra are in the conduction passageways and are therefore important to the conductivity of the material. Other I–O polyhedra are also important to the conductivity: 23.1%, or 12, of the Ag^+ ions are trapped in 12 of them and 32.4%, or 16.8, of the Ag^+ ions are in what we have called bypass sites (see Table V). The latter are not in conduction passageways but the Ag^+ ions in them could possibly be excited into conduction passageways. (It should be recalled that there are 28 empty I–O polyhedral sites, 16 of which are too close to filled sites, the remaining 12 being close, 2.9 to 3.2 Å, to W atoms.)

TABLE V

NET PERCENTAGE CONTENTS AND NET PERCENTAGE VOLUMES OF THE FOUR TYPES OF POLYHEDRA

Site type[a]	% Ag^+	% of unit cell volume	No. of sites/unit cell
$A(c)$	22.3	34.4	90
$AO(c)$	22.2	22.1	56
$AO(b)$	32.4	9.6	24
$AO(f)$	23.1	10.4	12

[a] Note: c, b, and f as defined in Table III.

The total number of sites per unit cell in the conduction passageways is 146, and the total number of mobile Ag^+ ions in these sites is 23.2 or 44.5% of the Ag^+ ions in the unit cell. The ratio of sites to Ag^+ ions in the conduction passageways is 6.3, a rather large value, comparable with that of α-AgI. The ratio of the total volume of the conduction passageways to that of the unit cell is 0.565, about half that of α-AgI, but comparable with that of $RbAg_4I_5$ (*6*, *8*). However, the average conductivity (Fig. 3) of $Ag_{26}I_{18}W_4O_{16}$ at 146°C is lower than those of both α-AgI and $RbAg_4I_5$. This may be attributed to the far more complicated conduction passageways in $Ag_{26}I_{18}W_4O_{16}$ and the lower mobilities through the I–O polyhedra.

Our conductivity measurements (Fig. 3) do not go to the melting point of the material.

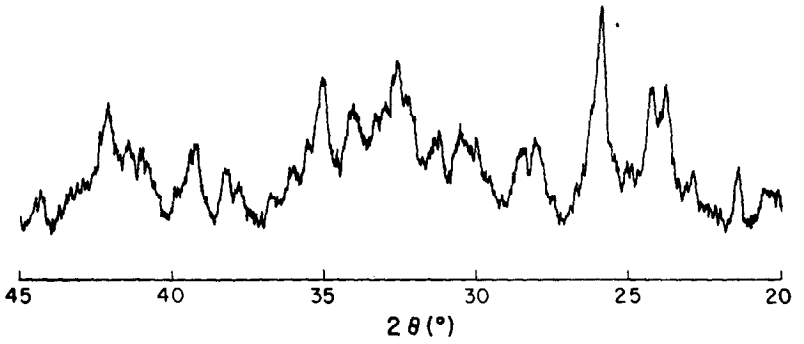

FIG. 10. Powder pattern of $Ag_{26}I_{18}W_4O_{16}$, Cu$K\alpha$ radiation.

Although the measurements made by Takahashi *et al.* (*11*) were not made on single phase material, the conductivity is associated essentially with the $Ag_{26}I_{18}W_4O_{16}$. Their σ vs T curve does not show any discontinuity or inflection up to the melting point. This indicates that the number of mobile Ag^+ ions probably does not increase markedly with increasing temperature (see Refs. *4*, *8*, *27*), although *some* increase from the bypass sites as a source is probably to be expected.

Finally, it should be mentioned that the iodide polyhedral network can alone provide the passageways for conduction. However, as shown in the previous section, the I–O polyhedra in conduction passageways provide shorter routes.

Appendix: Identification of $Ag_{26}I_{18}W_4O_{16}$

Inasmuch as the powder pattern (in the form of a list of d-values and qualitative relative intensities) given in the Takahashi *et al.* (*11*) paper is in considerable disagreement with that obtained for the pure material, we give, in this section, some information required to identify the polycrystalline material by the X-ray powder diffraction technique. Because of the complexity of the structure, we believe that it is futile to give a list of lines as is usually done. Therefore, we show in Fig. 10 a powder pattern taken with a Norelco diffractometer, using Cu$K\alpha$ radiation, in the range $20° < 2\theta < 45°$. In addition, using the parameters obtained from the structure analysis, we have calculated all the powder intensities in this range. These are obtainable (*27*) along with the list of F_{obs} vs F_{calc}.

To determine whether excess $Ag_{10}I_2W_4O_{16}$ is present, look for lines at $2\theta = 27.3$, 29.1, 30.2, 30.9, and 31.4°. These should not appear in the powder pattern of pure $Ag_{26}I_{18}W_4O_{16}$ (Fig. 10). They *do* appear in the powder pattern of material made according to the nominal formula $Ag_6I_4WO_4$.

The presence of γ-AgI is indicated by a *relative* increase in intensity at $2\theta = 23.7$ and 39.2° from the 111 and 220 reflections of γ-AgI, respectively.

Acknowledgments

We wish to thank S. A. Wilber and G. F. Ruse for technical assistance, Dr. J. L. Munoz of the Geological Sciences Department (University of Colorado) for use of the Norelco powder diffractometer, and Dr. A. Zalkin, Chemistry Department, Lawrence Berkeley Laboratory, U.C. Berkeley, and Dr. K. N. Raymond, Chemistry Department, U.C. Berkeley, for consultation on the use of the Lawrence Berkeley Computer facilities.

References

1. S. GELLER, *Science* **157**, 310 (1967).
2. S. GELLER AND M. D. LIND, *J. Chem. Phys.* **52**, 5854 (1970).
3. S. GELLER, *Science* **176**, 1016 (1972).
4. S. GELLER AND B. B. OWENS, *J. Phys. Chem. Solids* **33**, 1241 (1972).
5. S. GELLER AND P. M. SKARSTAD, *Phys. Rev. Lett.* **33**, 1484 (1974).
6. S. GELLER, P. M. SKARSTAD, AND S. A. WILBER, *J. Electrochem. Soc.* **122**, 332 (1975).

7. S. GELLER, *in* "Fast Ion Transport in Solids" (W. van Gool, Ed.), pp. 607–616, North–Holland/American Elsevier, Amsterdam/New York (1973).
8. S. GELLER, *in* "Superionic Conductors" (G. D. Mahan and W. L. Roth, Eds.), pp. 171–182, Plenum, New York/London (1976).
9. S. GELLER, *Phys. Rev. B* **14**, 4345 (1976).
10. H. WIEDERSICH AND S. GELLER, *in* "The Chemistry of Extended Defects in Non-Metallic Solids" (L. Eyring and M. O'Keefe, Eds.), pp. 629–650, North–Holland, Amsterdam (1970).
11. T. TAKAHASHI, S. IKEDA, AND O. YAMAMOTO, *J. Electrochem. Soc.* **120**, 647 (1973).
12. T. TAKAHASHI, S. IKEDA, AND O. YAMAMOTO, *J. Electrochem. Soc.* **119**, 477 (1972).
13. P. M. SKARSTAD AND S. GELLER, *Mater. Res. Bull.* **10**, 791 (1975).
14. By G. F. RUSE as reported in Ref. (13).
15. A. TURKOVIČ, D. L. FOX, J. F. SCOTT, S. GELLER, AND G. F. RUSE, *Mater. Res. Bull.* **12**, 189 (1977).
16. K. SHAHI AND S. CHANDRA, *Phys. Status Solidi (a) 28*. 653 (1975).
17. "International Tables for X-Ray Crystallography" (N. F. M. Henry and K. Lonsdale, Eds.), Vol. 1, Kynoch Press, Birmingham (1969).
18. P. B. CRANDALL, *Rev. Sci. Instrum.* **41**, 1895 (1970).
19. A. SCHUYFF AND J. B. HULSCHER, *Rev. Sci. Instrum.* **36**, 957 (1968).
20. W. L. BOND, *Rev. Sci. Instrum.* **22**, 344 (1951).
21. W. R. BUSING, K. O. MARTIN, AND H. A. LEVY, Oak Ridge National Laboratory Report ORNL-TM-305 (1962).
22. R. DOEDENS AND J. A. IBERS, NUCLS 8 (version of Ref. *21*).
23. S. GELLER, *Acta Crystallogr.* **14**, 1026 (1961).
24. D. T. CROMER AND J. T. WABER, *Acta Crystallogr.* **18**, 104 (1965).
25. M. TOKONAMI, *Acta Crystallogr.* **19**, 486 (1965).
26. D. T. CROMER, *Acta Crystallogr.* **18**, 17 (1965).
27. T. HIBMA, *Phys. Rev.* **B15**, (1977).